Physica B 404 (2009) 2730–2732

Contents lists available at ScienceDirect

Physica B

journal homepage: www.elsevier.com/locate/physb

Dynamical behavior of the phase transition of strained $BaTiO_3$ from atomistic simulations

Marcelo Sepliarsky [a], Silvia Tinte [b,*]

[a] Instituto de Física Rosario, Universidad Nacional de Rosario, 27 de Febrero 210 Bis, 2000 Rosario, Argentina
[b] INTEC, Universidad Nacional del Litoral, Güemes 3450, 3000 Santa Fe, Argentina

ARTICLE INFO

PACS:
77.55.+f
77.80.Bh
77.84.Dy

Keywords:
Ferroelectrics
Misfit strain
Atomistic simulations

ABSTRACT

Using an atomistic shell model we study the temperature dependence of the ferroelectric properties of $BaTiO_3$ under biaxial compressive strain applicable to growth on perovskites substrate. Molecular dynamics simulations show a "$r \rightarrow c \rightarrow p$" sequence of phase transitions when temperature is increased, and the absence of an "*ac* phase". The first-order paraelectric-to-ferroelectric phase transition presents in bulk changes to a second-order one as a consequence of the in-plane constraint imposed by the mechanical boundary conditions. From the tetragonal ferroelectric *c* phase, the transition takes place in a finite range of temperature where the lattice parameter normal to the plane keeps approximately constant until T_c is reached. Analysis of the local polarization behavior reveals an order–disorder dynamics as the dominant mechanism of the transition.

1. Introduction

Ferroelectric materials are attractive for device applications due to their ability to maintain a macroscopic polarization that can be switched by the application of an electric field [1]. They also exhibit a strong strain–polarization coupling [2] responsible for the changes in the paraelectric-to-ferroelectric transition temperature T_c, piezoelectric coefficients and dielectric properties when the mechanical boundary conditions are altered.

In the trend of decreasing the size of electronic devices, ferroelectrics in the thin film form have drawn attention, but their properties might differ significantly than those in bulk. One of the main factors that contributes to that difference is the misfit strain imparted by the substrate on the film, which can be exploited to enhance particular properties, namely strain engineering [3]. For example, using molecular beam epitaxy and pulsed laser deposition, thin films of the prototypical ferroelectric perovskite $BaTiO_3$ (lattice constant of 4.00 Å) were biaxially grown on $GdScO_3$ (lattice constant of 3.965 Å) and also on $DyScO_3$ (lattice constant of 3.943 Å); it was found that T_c and the remanent polarization were much higher than in bulk $BaTiO_3$ [4]. It was also shown that the phase-transition nature changes to second order with respect to the first-order transition in the bulk crystal.

Theoretical approaches, including first principles and thermodynamics analysis, were used to describe temperature-versus-misfit strain "Pertsev" phase diagrams for thin films of a number of ferroelectrics including $BaTiO_3$ [5,6]. In particular in these works, a single and homogeneous domain state was assumed, whereas surface and domain effects were neglected. Thus, these diagrams that map equilibrium structures versus temperature and epitaxial strain were obtained simulating the bulk material with an homogeneous strain tensor constrained to a square surface symmetry. Although they give useful information about epitaxial phases, these studies do not address the question of how the nature of the phase-transition dynamics is affected by epitaxial strain.

In this work, we study the temperature evolution and the underlying dynamical behavior of $BaTiO_3$ under a particular compressive epitaxial strain by using an atomic level model. We first present the computational details and then the temperature dependence properties. Finally, we analyze the nature of the local dynamics related to the phase transitions.

2. Model and computational details

We use here an atomistic shell model for $BaTiO_3$ that was originally developed to study bulk properties in $Ba_xSr_{1-x}TiO_3$ solid solutions [7]. In the model, each atom is described as a core linked to a massless shell through an anharmonic spring with potential $V(w) = \frac{1}{2}k_2w^2 + \frac{1}{24}k_4w^4$, with w the core–shell displacement, and k_2 and k_4 parameters. The model also considers long-range Coulombic interaction among cores and shells of different atoms, and short-range interaction between shells of the pairs: Ba–O, Ti–O and O–O. For the last case, the interaction is described by a Buckingham potential $V(r) = Ae^{(-r/\rho)} - C/r^6$ with parameters

* Corresponding author. Tel.: +54 342 4559174; fax: +54 342 4550944.
E-mail address: tinte@intec.unl.edu.ar (S. Tinte).

0921-4526/$ - see front matter © 2009 Elsevier B.V. All rights reserved.
doi:10.1016/j.physb.2009.06.079

A, ρ, C. The model parameters were fitted to reproduce the underlying potential energy surfaces for ferroelectric distortions and optimized crystal structures. The initial parameters were taken from a shell model fitted to density functional theory (DFT) calculations [8]. That former model was able to properly describe the non-trivial phase sequence in bulk $BaTiO_3$, but the predicted transition temperatures were much lower than the experimental ones. To overcome that deficiency, the present potential parameters were improved in an *ad hoc* manner to obtain a better agreement, as described in Ref. [7].

In our calculations the substrate is not explicitly simulated, only bulk $BaTiO_3$ under fix in-plane strain is considered. Our results correspond to one particular misfit strain, $\eta_s = a/a_0 - 1$, of -1.25×10^{-2} where a_0 is the $T = 0$ lattice constant of bulk $BaTiO_3$ (4.01 Å) as computed using this approach.

To explore properties at finite temperatures we perform molecular dynamics (MD) simulations at constant number of particles, temperature and misfit strain. In practice, for each temperature the in-plane lattice parameters are fixed, $\mathbf{a}_1 = a\hat{x}$ and $\mathbf{a}_2 = a\hat{y}$, along the simulation while only the perpendicular component, $\mathbf{a}_3 = c\hat{z}$, is allowed to relax by doing zero the $z-z$ stress-tensor component through a Berensden approach. The temperature dependence of the in-plane lattice parameters is arbitrary in calculations; here for simplicity we impose by hand the bulk thermal expansion obtained in the tetragonal phase. However, note that experimentally a strained system will naturally expand following the substrate thermal expansion where it was grown. MD runs were performed in a $8 \times 8 \times 8$ unit-cell supercell with periodic boundary conditions. The time step was set to 0.4 fs, and results at each temperature were collected for at least for 80 000 MD steps after equilibration of 20 000 MD steps.

3. Results

The behavior of epitaxial $BaTiO_3$ changes significantly with respect to bulk. Fig. 1(a) shows the temperature dependence of the lattice constant components under a biaxial strain, while the behavior of the spontaneous polarization components are displayed in Fig. 1(b), both with filled symbols. The corresponding bulk values are also included in both figures for comparison using open symbols. One can clearly see that the fix in-plane strain mimicking a substrate replaces the four phases present in bulk $BaTiO_3$ (three ferroelectrics: rhombohedral, orthorhombic and tetragonal, and one cubic paraelectric) by the following three phases. One ferroelectric monoclinic r phase at the lowest temperatures having polarization components $P_x = P_y \neq P_z$, a ferroelectric tetragonal c phase for intermediate temperatures with polarization P_z, and one paraelectric p state at high temperatures. Specifically at $T = 0$ K, the imposed in-plane compression of -1.25% is compensated by an expansion of the perpendicular lattice constant of 2.4%. Whereas P_x and P_y decrease to 9 $\mu C/cm^2$ and P_z increases to 27 $\mu C/cm^2$ with respect to the three equal polarization components of 16.1 $\mu C/cm^2$ in bulk. As temperature increases, the r phase exists until 50 K where P_x and P_y vanish simultaneously indicating a $r \rightarrow c$ transition, but no appreciable change in the lattice constants is observed from our calculations. As such a small temperature range of existence of the r phase does not allow us to analyze it in detail, hereafter we will focus only on the c phase. As the temperature is further increased, $\mathbf{a}_3$ expands thermally and P_z remains nearly constant until ~600 K. At this temperature, P_z starts decreasing gradually until vanishes finally at T_c~800 K, in contrast to the abruptly drop seen in bulk. Furthermore, in this region $\mathbf{a}_3$ keeps almost constant and does not show a discontinuity at T_c. These features are a clear signature of a second-order phase transition, in agreement with experimental results reported in compressive strained $BaTiO_3$[4], and differ from the first-order nature observed in bulk. Finally, above T_c in the p state, $\mathbf{a}_3$ recovers the thermal expansion.

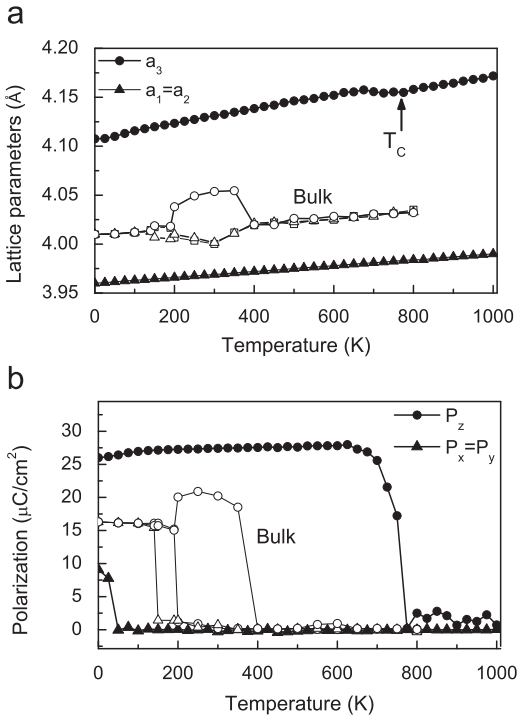

Fig. 1. Phase diagram of epitaxial $BaTiO_3$ (filled symbols): (a) lattice parameter components and (b) spontaneous polarization components. For comparison the phase diagram of bulk $BaTiO_3$ is also shown using open symbols.

The simulated phase diagram of epitaxial $BaTiO_3$ is consistent with other theoretical descriptions and experimental results. In particular, the obtained sequence of phase transitions $r \rightarrow c \rightarrow p$ is in excellent agreement with the results displayed at the same misfit strain in the Pertsev-phase diagram obtained using a first-principles model Hamiltonian [6]. Interestingly, no *ac phase* ($P_x \neq 0, P_y = 0, P_z \neq 0$) was observed in our simulations as was originally proposed using a phenomenological theory [5], but later discarded with first-principles calculations [6]. That phase would be related to the bulk orthorhombic one, however, the absence of in-plane relaxation frustrates its stability producing a direct $r \rightarrow c$ transition, as found here. On the other hand, the low value of the lowest transition temperature is in coincidence with Ref. [6], and suggests proximity to a c phase under an increment in the compressive strain; whereas our T_c value is ~300 K higher than the reported one in that work. Note that T_c is in the range of the expected experimental value [4] showing the ability of our model to predict transition temperature closer to the experimental ones.

Now we turn our attention to the underlying microscopic behavior of the ferroelectric-to-paraelectric phase transition. To explore its dynamics, we choose the local polarization with components p_i as the order parameter, defined here as the polarization of a single perovskite cell centered at the Ti ion. We have identified that strained $BaTiO_3$ presents three different regimes of dynamical behavior as a function of temperature. Fig. 2 shows local-polarization distribution functions [9] for each region, and the inset displays the time evolution of p_z for one particular single cell at the corresponding temperatures. In the low temperature regime ($T \leq 600$ K), the polarization of each cell displays fast oscillations around a finite value $+p_z = 27.8\ \mu C/cm^2$ as shown in the inset, which results in an unimodal distribution

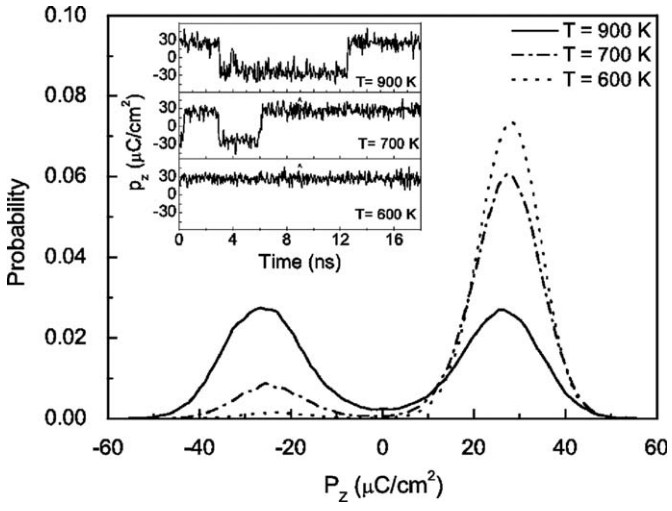

Fig. 2. Polarization distribution function at three temperatures corresponding to different dynamical regions. The inset shows the time evolution of a cell polarization in the same regions.

(dotted line). Accordingly, P_z remains approximately constant in this region as observed in Fig. 1(b). In the intermediate region ($600\,K < T < 800\,K$), a new component in the dynamics appears: in addition to the oscillations around one equilibrium value $+p_z$, some cells are able to jump (back and forward) to other equilibrium value at $-p_z$ with a much slower relaxation time. This behavior starts in some non-correlated unit cells around 600 K, and becomes present in an increasing number of cells as the temperature goes up. Thus, a second peak shows up in the distribution which grows as temperature increases reducing the $+p_z$ peak, i.e., the distribution turns bimodal (dot-dashed line). Indeed, the difference in height of these peaks is responsible for the gradual dropping of P_z seen in Fig. 1(b). Since polarization jumps occur in longer period of time with respect to the oscillations, more MD steps are required in the simulations in order to obtain a good statistic. Nevertheless, we have found that the behavior of this region does not change increasing the simulation time. Finally, above T_c all unit cells show the coexistence of the two types of motion with different time scales, the p_z distribution become symmetric (solid line), and then the average P_z vanishes. Thus, this detailed description indicates us that the ferroelectric-to-paraelectric transition in strained $BaTiO_3$ has mainly an order–disorder character. Regarding the in-plane components of local polarization, p_x and p_y do not exhibit any anomaly at this high temperature T_c showing a unimodal distribution centered at zero.

Our simulations show that the paraelectric-to-ferroelectric phase transition in strained $BaTiO_3$ displays an order–disorder character. Although the behavior is similar to what is found in bulk, we can notice two main changes in the dynamics produced by the strain. The first one is related to the local behavior. In bulk, each Ti ion can occupy one of the eight off-center equivalent positions along the body diagonals of the cell in all phases [10], which will determine the local-polarization direction [11–13]. According to this, the phase transitions can be described in terms of the population of equivalent sites, as it is done using an eight site model [14]. In strained $BaTiO_3$ there are also eight equivalent polar directions at $T = 0\,K$, however, simulations show that local polarizations oscillate between two equivalent sites, $(0, 0, +p_z)$ and $(0, 0, -p_z)$, in the paraelectric phase, and around only one site in the c-phase below T_c. These results suggest that the transition temperature is high enough to wash out the in-plane difference between sites. In fact, the picture of an eight site model description (distorted by the strain) is recovered at low temperatures in the same c-phase just before the transition to the r-phase, i.e., below 100 K, p_x and p_y start to display a bimodal distribution. We want to remark here that the present description is valid for large compressive in-plane strain values, and a different behavior could be expected for strains in a different range. The second difference with respect to bulk is related to the character of the transition. It changes from first-order in bulk to second-order in the strained system, which is in complete agreement with experiments [15,16]. Since the reported experimental results are at different misfit strain, the change in the character should be related to the clamping of the in-plane lattice parameters. Ferroelectric transitions are very sensitive to the homogeneous strain, and one can infer that the fix in-plane lattice parameters do not allow the cell deformation required to obtain a sharp stabilization of the polarization. On the other hand, our results also probe that the nature and type of transition reported here are intrinsic effects of the compressive misfit strain, and not a consequence of other factors such as surfaces, inhomogeneous strain or defects. Finally, based on the observed slowing down in the relaxation dynamics of local polarizations in the transition region, we suggest that this behavior is probably responsible for the strong frequency dispersion of the dielectric permittivity seen in epitaxial $BaTiO_3$ films [16].

In summary, using an atomistic shell model for $BaTiO_3$ under compressive misfit strain we find a sequence of phase transitions $r \rightarrow c \rightarrow p$ as a function of temperature, as reported using a first-principles model Hamiltonian for the same strain value. Importantly our model reproduces the second-order phase transition in agreement with experimental results, and indicates that order–disorder is the dominant dynamics mechanism for the $c \rightarrow p$ phase transition.

Acknowledgment

This work was supported by the Agencia Nacional de Promoción Científica y Técnica de la República Argentina (PICT2006-1985).

References

[1] M. Dawber, K.M. Rabe, J.F. Scott, Rev. Modern Phys. 77 (2006) 1083.
[2] R.E. Cohen, Nature (London) 358 (1992) 136.
[3] D.G. Schlom, L.-Q. Chen, Ch.-B. Eom, K.M. Rabe, S.K. Streiffer, J.-M. Triscone, Annual Rev. Mater. Res. 37 (2007) 589.
[4] K.J. Choi, M. Biegalski, Y.L. Li, et al., Science 306 (2004) 1005.
[5] N.A. Pertsev, A.G. Zembilgotov, A.K. Tagantsev, Phys. Rev. Lett. 80 (1998) 1988.
[6] O. Diéguez, S. Tinte, A. Antons, C. Bungaro, J.B. Neaton, K.M. Rabe, D. Vanderbilt, Phys. Rev. B 69 (2004) 212101.
[7] S. Tinte, M.G. Stachiotti, S.R. Phillpot, et al., J. Phys. Condens. Matter 16 (2004) 3495.
[8] S. Tinte, M.G. Stachiotti, M. Sepliarsky, et al., J. Phys. Condens. Matter 11 (1999) 9679.
[9] These distributions are histograms that result of accumulating snapshots of all the local p_z values in the simulation supercell every 40 fs in a total simulation time of 40 ps.
[10] B. Zalar, V.V. Laguta, R. Blinc, Phys. Rev. Lett. 90 (2003) 037601.
[11] W. Zhong, D. Vanderbilt, K.M. Rabe, Phys. Rev. Lett. 73 (1994) 1871.
[12] S. Tinte, M.G. Stachiotti, M. Sepliarsky, R.L. Migoni, C.O. Rodriguez, Ferroelectrics 237 (2000) 41.
[13] M.I. Marqués, Phys. Rev. B 71 (2005) 174116.
[14] A.S. Chaves, F.C.S. Barreto, R.A. Noguera, B. Zeks, Phys. Rev. B 13 (1976) 207.
[15] M. El Marssi, F. Le Marrec, I.A. Lukyanchuk, M.G. Karkut, J. Appl. Phys. 94 (2003) 3307.
[16] M. Tyunina, J. Levoska, I. Jaakola, Phys. Rev. B 75 (2007) 140102.